Journal of Thermal Analysis, Vol. 48 (1997) 177-202

Dedicated to Dr. Robert Mackenzie on the occasion of his 75th birthday

APPLICATION OF THERMAL ANALYSIS TO MINERAL SYNTHESIS

A. M. Abdel-Rehim

Mineral Engineering Laboratory, Alexandria University, Egypt

Abstract

Differential thermal analysis (DTA) and thermogravimetry (TG) are applied to various fields of mineral science. The present work illustrates the importance of the application of thermal analysis to mineral synthesis, to the determination of the mechanism and optimum temperature of synthesis and the thermal behaviour of minerals and starting materials. Selected examples of applications in this field are given. These include DTA studies of the synthesis of topaz, cryptohalite, wulfenite, perovskite, scheelite and the refractory materials, baddeleyite and corundum.

Thermal analysis is proved to be an important and valuable tool in mineral synthesis.

Keywords: DTA, mineral synthesis, TG

Introduction

Differential thermal analysis (DTA) and thermogravimetry (TG) are applied to various fields of mineral science. These include mineralogy, thermoanalytical testing of minerals, mineral synthesis, industrial processing of minerals, manufacture of ceramics, glass, refractories, cement, fluxes, mineral pigments, chemical industry and metallurgical processes [1–12, 18, 20].

Chemical analysis can provide hardly any information on the mineral composition of ores, rocks, soils and clays. X-ray analysis is tedious, because of the overlapping of the interference lines, especially if a minor component is to be detected. In thermoanalytical investigations, physical and chemical transformations of minerals appear clearly. Hence, DTA may be applied to the identification and determination of mineral constituents and may provide more accurate results than other methods. Extensive DTA studies were carried out on the dehydration of clays, mineral composition of bauxites, thermal decomposition of carbonate and sulphate minerals, sulphides, coal, coke, lignites, peats, their burning process and mechanism of gasification [9, 12, 18, 20].

The present work illustrates the importance of application of thermal analysis to mineral synthesis, to the determination of the mechanism and optimum temperature

0368–4466/97/ $ 5.00

John Wiley & Sons Limited

Chichester

of synthesis and the thermal behaviour of the produced minerals and starting materials. This work will cover selected examples of the application of DTA to mineral synthesis.

Experimental

Apparatus

The experiments were carried out using platinum crucibles, heated in an electrical furnace with removal of the evolved gases & vapours which resulted from the reaction. The temperature was regulated automatically with an accuracy of ±5°C.

Thermal studies of mineral syntheses were carried out by using a derivatograph (MOM, Hungary) [20]. This apparatus records simultaneously four curves: the change of temperature of the sample (T), differential thermal analysis (DTA), thermogravimetric (TG) and the derivative thermogravimetric (DTG) curves on a single sample under controlled conditions.

The parameters during the test were as follows: Platinum crucible, medium size; inert material; aluminium oxide; weight of sample ranging from 0.5 to 1 g; temperature range from ambient up to 1200°C; weight used in TG analysis: 100, 500, 1000 mg; heating rate 10°C min^{-1}. Pt-Pt/Rh thermocouples were used for the DTA and temperature measurements. The atmosphere was air and the volatiles were removed as formed.

Phase identification

X-ray procedure. The phases of the products of mineral syntheses were identified both microscopically and by X-ray diffraction analysis using a Siemens Cristalloflex D 500 diffractometer. The finely ground product was mixed with sodium chloride as a standard. Its peaks occurring at $2\theta=31.38°$ and 45.44° were used for corrections. Nickel-filtered copper radiation was used. Exposure time was 1 h. Intensities were collected to maximum $2\theta=80°$. The sensitivity of the experiment was 4×10^4 impl./min and the statistical error was 1.5%.

Results and discussion

Synthesis of baddeleyite from zircon

Baddeleyite (ZrO_2) can be synthesized from zircon by its sintering with aluminium fluoride [1, 4, 9]. The DTA curve of a mixture of zircon with aluminium fluoride of an amount 150% of the theoretical value and graphite in an amount 10% of zircon is shown in Fig. 1. The three endothermic peaks at 105, 315 and 450°C agree with the thermal data of aluminium fluoride. The exothermic peak at 580°C represents the burning of graphite and the slow reaction of desilication of zircon and combustion of volatiles. The desilication of zircon with aluminium fluoride takes place intensively at 820°C as indicated by the large endothermic peak at this temperature. This process is accompanied by a sharp decrease in weight (TG) due

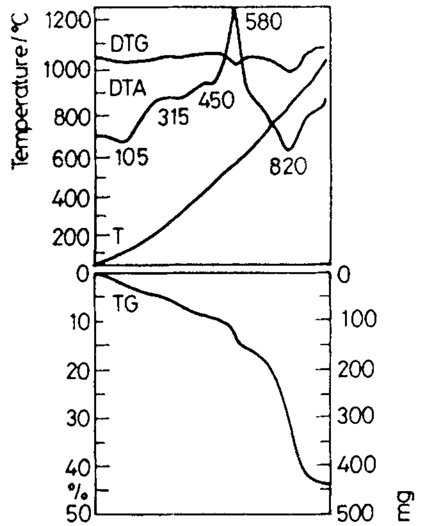

Fig. 1 DTA curve of the synthesis of baddeleyite by sintering zircon with aluminium fluoride in the presence of graphite. Weight of sample 1000 mg, heating rate 10°C min^{-1}

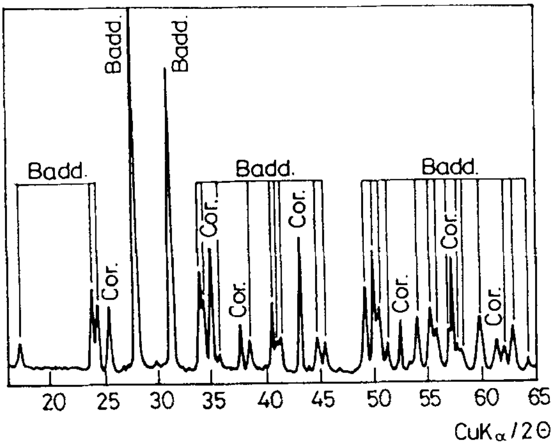

Fig. 2 X-ray diffraction pattern of the product of the sintering of zircon with aluminium fluoride. Badd. = baddeleyite and Cor. = corundum

to the volatilization of silicon tetrafluoride. The desilication of zircon results in the production of baddeleyite and corundum (Fig. 2), which are suitable for refractory purposes. The old methods of production of high zirconium refractory materials, baddeleyite and corundum included several stages. Zircon should be converted to the oxide and then mixed with aluminium oxide. The different chemical processing methods of zircon [17, 22], include sintering of zircon with soda or alkali and leaching with alkali solutions.

The desilication of zircon with aluminium fluoride with direct production of baddeleyite and corundum takes place according to:

$$3ZrSiO_4+4AlF_3 \rightarrow 3ZrO_2+2Al_2O_3+3SiF_4$$

baddeleyite corundum

The standard free energy (ΔF^0) and the equilibrium constant of this reaction (K) were estimated to be –83.2 kcal mol^{-1} and 9.68×10^{60}, respectively.

Synthesis of cryptohalite

Cryptohalite (Ammonium silicon hexafluoride) occurs as a sublimation product at the Vesuvius volcano and coal seams [10, 21].

Cryptohalite can be synthesized by sintering quartz with ammonium fluoride [10]. The DTA curves (Fig. 3A and B) show the formation of cryptohalite as shown by the wide and sharp endothermic peak at 150°C. The small endothermic peak at 230°C represents the dissociation of the resulted ammonium bifluoride. The large and sharp endothermic peak at 320–335°C represents the intensive dissociation of cryptohalite. These processes are connected with a sharp decrease in weight (TG curve) due to the volatilization of silicon tetrafluoride and removal of ammonia, hydrogen fluoride and water vapours. The small endothermic peak at 570°C represents the phase transformation of alpha-quartz to the beta-form.

The DTA curve of quartz mixed with 150% of the theoretical amount of ammonium fluoride (Fig. 3B) shows similar peaks at similar temperatures as that obtained using 100% of the theoretical amount of ammonium fluoride with the exception of the disappearance of the wide and sharp endothermic peak at 150°C. This

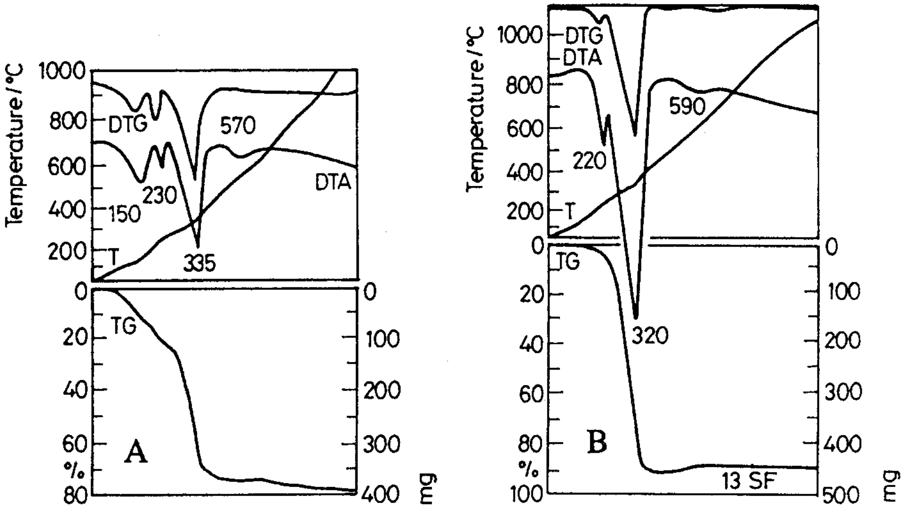

Fig. 3 DTA curves of the synthesis of cryptohalite by sintering quartz with ammonium fluoride of theoretical amount (A) and with 150% of the theoretical amount (B), respectively. Weight of sample 500 mg, heating rate 10°C min^{-1}

may be attributed to the dissociation reaction of the resulted ammonium bifluoride covering the formation reaction of cryptohalite.

The X-ray diffraction patterns of the products at 150 and 200°C (Fig. 4A and B) respectively show the presence of cryptohalite at 150°C and its association with the double compound ($(NH_4)_2SiF_6{\cdot}NH_4F$) at 200°C.

The mechanism of the reaction of cryptohalite synthesis by sintering quartz with ammonium fluoride can be described as follows:

At 150°C: The reaction of quartz with ammonium fluoride takes place with the formation of cryptohalite.

$$\underset{\text{quartz}}{SiO_2}+6NH_4F \rightarrow \underset{\text{cryptohalite}}{(NH_4)_2SiF_6}+4NH_3+2H_2O$$

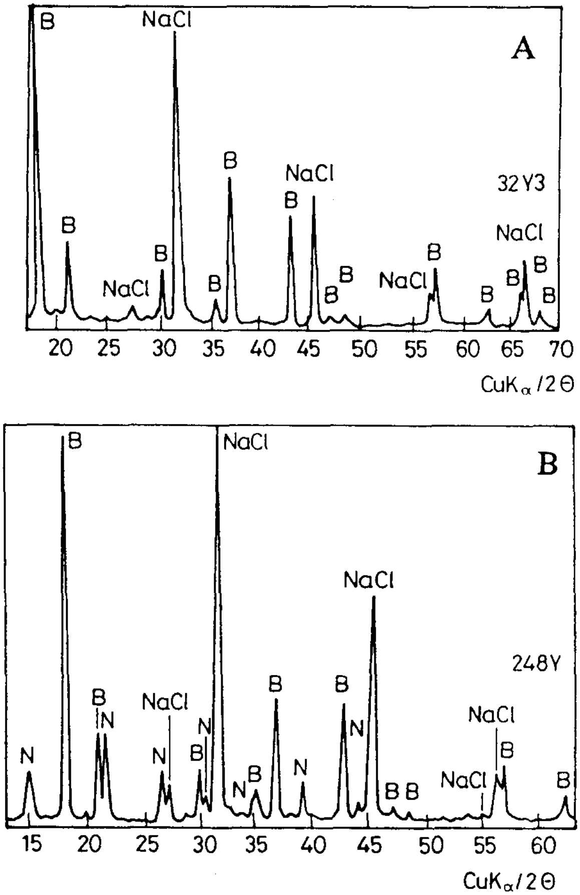

Fig. 4 X-ray powder diffraction patterns of the products of synthesis of cryptohalite using quartz mixed with 150% the theoretical amount of ammonium of fluoride. (A) and (B) at 150 and 200°C respectively. B=cryptohalite, N=$(NH_4)_2SiF_6{\cdot}NH_4F$

At 200°C and with excess ammonium fluoride: The reaction of quartz with ammonium fluoride takes place with the formation of cryptohalite and a double compound.

$$\underset{\text{quartz}}{2SiO_2}+13NH_4F \rightarrow \underset{\text{cryptohalite}}{(NH_4)_2SiF_6}+(NH_4)_2SiF_6\cdot NH_4F+8NH_3+4H_2O$$

At 320–335°C: Cryptohalite and the double compound $(NH_4)_2SiF_6\cdot NH_4F$ are unstable and dissociate according to:

$$\underset{\text{cryptohalite}}{(NH_4)_2SiF_6}+(NH_4)_2SiF_6\cdot NH_4F \rightarrow 2SiF_4+5NH_3+5HF$$

The synthesized cryptohalite is colourless in thin sections and crystallizes in the cubic system in the form of octahedral crystals with perfect (111) cleavage.

Synthesis of wulfenite

Wulfenite (lead molybdate) occurs as a secondary mineral in the oxidation zones of lead deposits, often associated with cerussite, galena, anglesite, pyromorphite, vanadinite and other minerals [11, 15, 21].

Synthesis of wulfenite by the sintering of molybdite with cerussite

The DTA curve of a 1:1 molybdite-cerussite mixture (Fig. 5) shows the characteristic peaks of cerussite. The sharp endothermic peak at 300°C represents the dehydration of hydrocerussite and the endothermic peak at 350°C represents the first step of cerussite dissociation into $PbO\cdot PbCO_3$. The second step of its dissociation into lead oxide is represented by the medium endothermic peak at 400°C. These

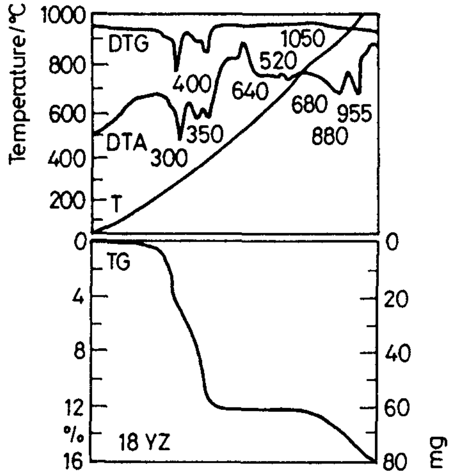

Fig. 5 DTA curve of the synthesis of wulfenite by sintering molybdite with cerussite. Weight of sample 500 mg

processes are connected with a sharp decrease in weight (TG curve) in steps. The first is the loss of constitutional OH radicals of hydrocerussite due to its dehydration and the second is the liberation of carbon dioxide resulted by dissociation of cerussite.

The formation of wulfenite takes place at 520°C as indicated by the exothermic peak at this temperature. The reaction of molybdenum and lead oxides was reported to take place at 500–600°C with the formation of lead molybdate [17, 22].

The medium endothermic peaks at 880 and 955°C represent the melting and vaporization of unreacted lead and molybdenum oxides. The small endothermic peak at 1050°C is due to the melting of the produced wulfenite. This is consistent with literature data [15, 17, 22] for the melting of lead molybdate at 1050–1065°C.

The X-ray diffraction patterns of the products at 520 and 955°C are shown in Fig. 6 A and B, respectively. At 955°C the whole product is wulfenite. Molybdite and lead oxide peaks disappear completely.

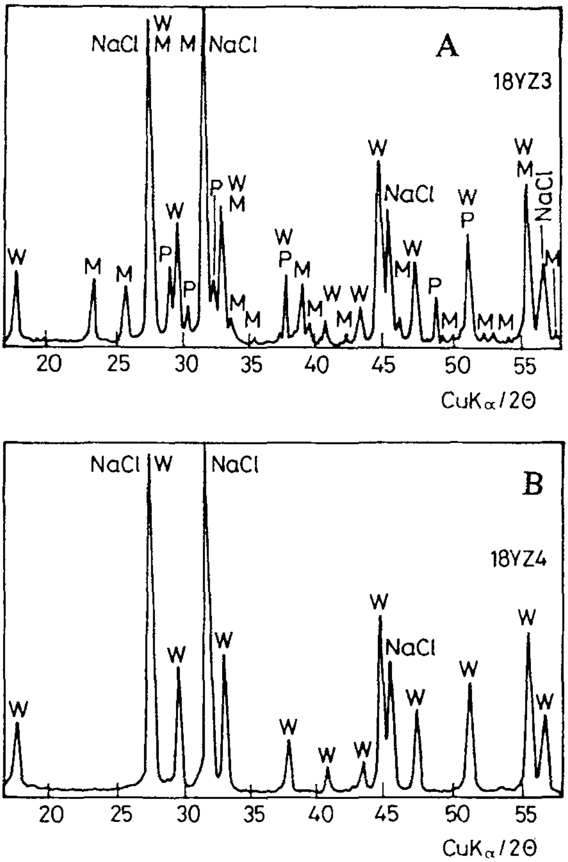

Fig. 6 X-ray powder diffraction patterns of the products of the synthesis of wulfenite by sintering molybdite with cerussite. (A) and (B) at 520 and 955°C, respectively. C=cerussite, M=molybdite, P=lead oxide and W=wulfenite

Synthesis of wulfenite by the sintering of molybdite with lead oxide

The DTA curve (Fig. 7) shows the formation of wulfenite at 500°C, as represented by the exothermic peak at this temperature. The melting and volatilization of unreacted lead and molybdenum oxides appear as only one large and sharp endothermic peak at 980°C. The TG curve shows a remarkable decrease in weight, due to volatilization. The small endothermic peak at 640°C may represent the beginning of vaporization of the oxides.

The resulted wulfenite is pale yellow in thin sections and crystallizes in the tetragonal system in the form of tabular crystals with distinct (011) cleavage.

The mechanism of synthesis of wulfenite by sintering molybdite with cerussite can be assumed to be as follows:

At 350°C, the first stage of dissociation of cerussite takes place according to:

$$\underset{\text{cerussite}}{2PbCO_3} \rightarrow PbO{\cdot}PbCO_3 + CO_2$$

At 400°C, the second stage of its dissociation takes place with the formation of lead oxide.

$$PbO{\cdot}PbCO_3 \rightarrow 2PbO + CO_2$$

At 500–520°C, the reaction of molybdite with lead oxide takes place with the formation of wulfenite.

$$\underset{\text{molybdite}}{MoO_3} + PbO \rightarrow \underset{\text{wulfenite}}{PbMoO_4}$$

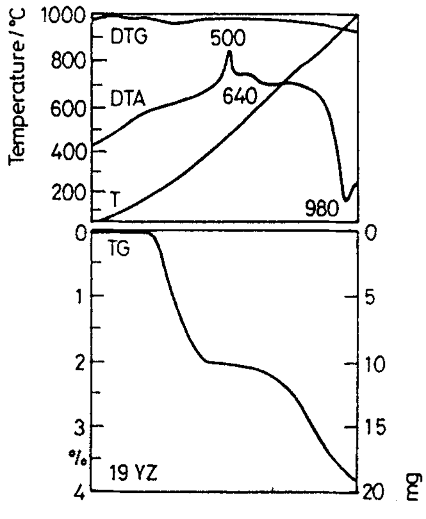

Fig. 7 DTA curve of the synthesis of wulfenite by sintering molybdite with lead oxide. Weight of sample 500 mg

The standard free energy (ΔF^0) and the equilibrium constant (K) of the reaction of wulfenite formation were estimated to be -22.04 kcal mol^{-1} and 1.43×10^{16}, respectively.

Synthesis of topaz

Topaz $Al_2[SiO_4]$ $(F,OH)_2$ occurs in high temperature quartz veins, pegmatites, granites, contact zone and associated with late-stage pneumatolytic action [8, 9, 21].

Topaz can be synthesized using different starting materials [2, 3, 8, 9, 13, 14], as kaolinite-aluminium fluoride mix, corundum-quartz mix with ammonium fluoride, kaolinite-ammonium fluoride mix and quartz-aluminium fluoride mix.

Synthesis of topaz by the sintering of kaolinite with aluminium fluoride

The DTA curve of synthesis of topaz by sintering a 1:1.3 mixture of kaolinite and aluminium fluoride is shown in Fig. 8. The first two wide and large endothermic peaks at 130 and 320°C are in good agreement with the thermal data of aluminium fluoride, representing its dehydration. The wide endothermic peak at 625°C represents the dehydration of kaolinite and its reaction with aluminium fluoride with the formation of topaz and mullite. The intensive formation of topaz is represented by the medium and sharp endothermic peak at 750°C.The very small endothermic peak at 800°C represents the property of topaz to lose silicon tetrafluoride [2, 13, 14].

The large and sharp endothermic peak at 950°C represents the dissociation of topaz and its desilication in the presence of excess aluminium fluoride with the for-

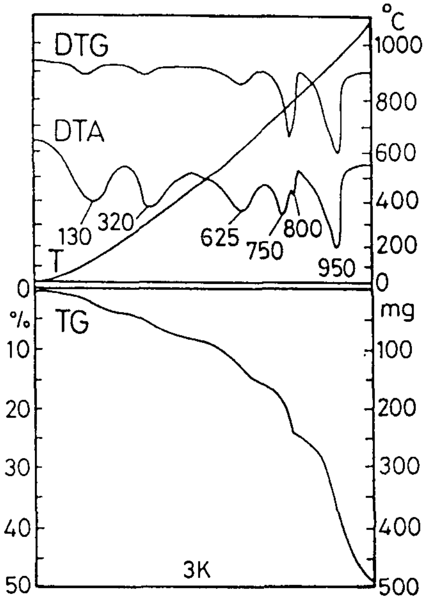

Fig. 8 DTA curve of the synthesis of topaz by sintering kaolinite-aluminium fluoride mix of a ratio of 1:1.3. Weight of sample 1000 mg; heating rate 10°C min^{-1}

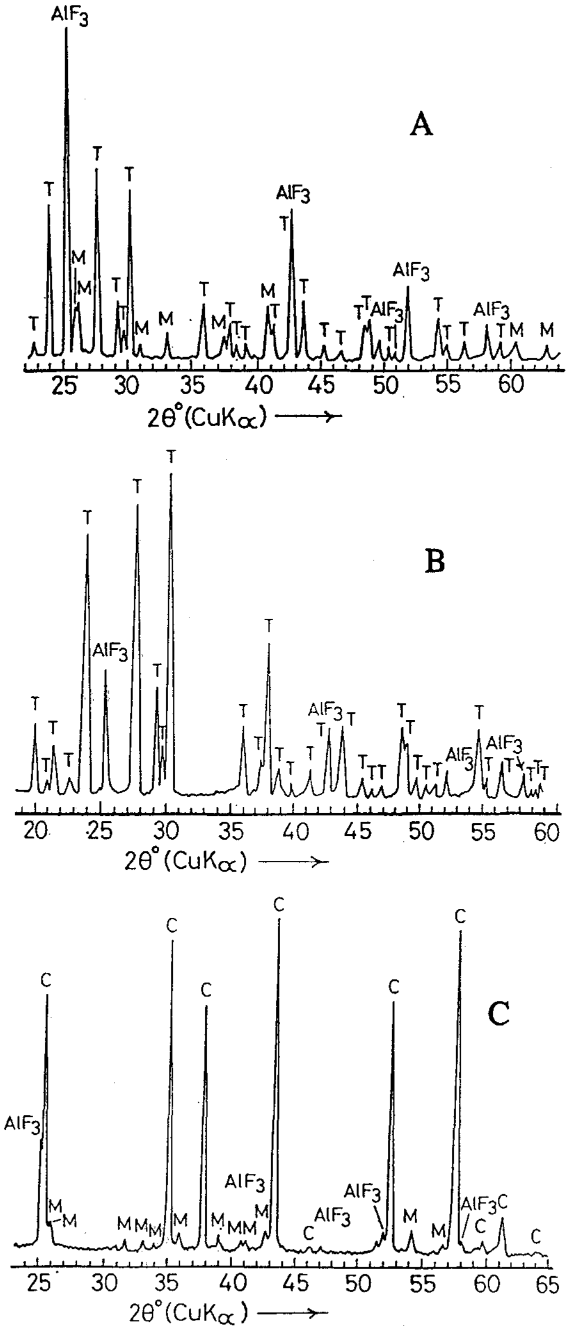

Fig. 9 X-ray powder diffraction patterns of the products of the synthesis of topaz using kaolinite-aluminium fluoride mix of a ratio of 1:1.3 (A), (B) and (C) at 600, 750 and 950°C, respectively. T=topaz, M=mullite and C=corundum

mation of corundum or alpha-aluminium oxide. This process is accompanied by a sharp decrease in sample weight (TG curve) due to the removal of silicon tetrafluoride and the loss of constitutional OH radicals.

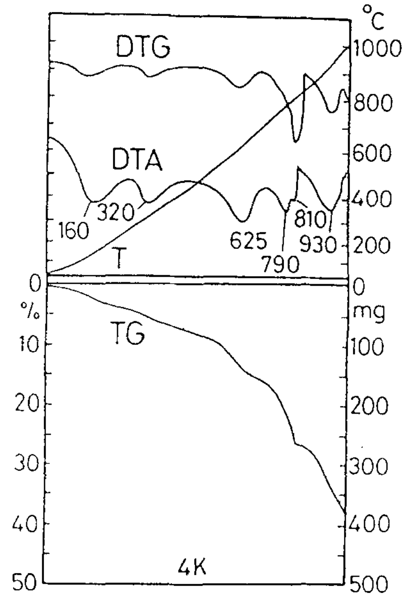

Fig. 10 DTA curve of the synthesis of topaz by sintering kaolinite-aluminium fluoride mix of a ratio of 1:0.7. Weight of sample 1000 mg, heating rate 10°C min^{-1}

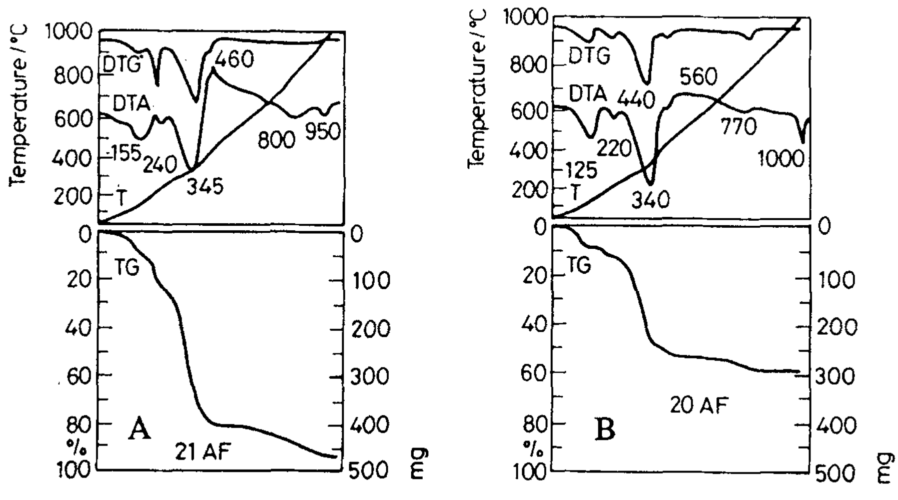

Fig. 11 DTA curves of the synthesis of topaz using corundum-quartz-ammonium fluoride mix of ratios of 1:1:6.4 (A) and 1:1:2.5 (B), respectively. Weight of sample 500 mg, heating rate 10°C min^{-1}

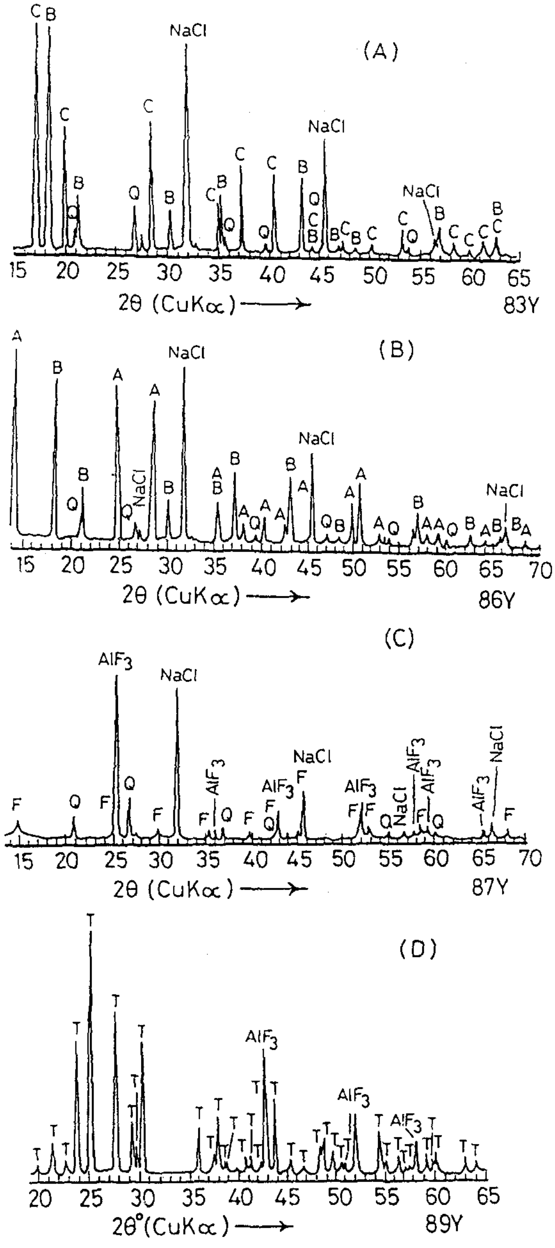

Fig. 12 X-ray powder diffraction patterns of the products of the synthesis of topaz using corundum-quartz-ammonium fluoride mix of a ratio of 1:1:6.4 (A), (B), (C), (D) and (E) at 155, 240, 345, 800 and 950°C, respectively. A=NH_4AlF_4; B=$(NH_4)_2SiF_6$ (cryptohalite), C=$(NH_4)_3AlF_6$, T=topaz; C=corundum; Q=quartz

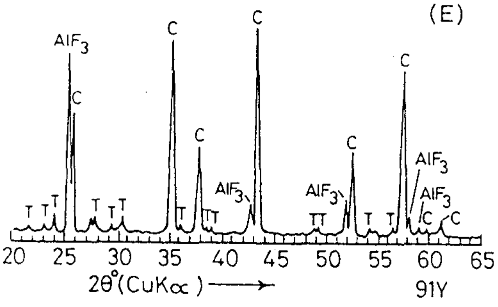

Fig. 12 Continued

The X-ray diffraction patterns of these products are shown in Fig. 9 (A at 600°C, B at 750°C and C at 950°C). The product at 600°C is composed mainly of topaz with some mullite. Topaz is the whole-product at 750°C and its peaks completely disappear in the run at 950°C. Corundum is the main product at 950°C.

The DTA curve of kaolinite mixed with aluminium fluoride in a ratio of 1:0.7 (Fig. 10) shows the formation of topaz at somewhat higher temperature than the previously recorded curve as shown by the endothermic peak at 790°C. The wide and large endothermic peak at 930°C indicates the dissociation of topaz with the formation of mullite as end product, due to the absence of aluminium fluoride, which is consumed in the formation of topaz.

Synthesis of topaz using corundum-quartz mixtures with ammonium fluoride

Thermal analysis data of the synthesis of topaz using corundum-quartz-ammonium fluoride mixtures with ratios of 1:1:6.4 and 1:1:2.5 [8, 9], are shown in Fig. 11A and B, respectively. The first wide and large endothermic peak at 125–155°C represents the formation of ammonium aluminium hexafluoride and ammonium silicon hexafluoride (Cryptohalite). The small endothermic peak at

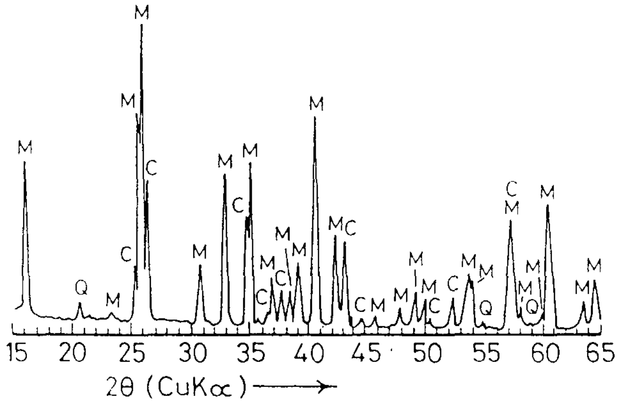

Fig. 13 X-ray powder diffraction pattern of the product of the synthesis of topaz using mixes of corundum-quartz-ammonium fluoride of a ratio of 1:1:2.5 at 1000°C. C=corundum, M=mullite, T=topaz and Q=quartz

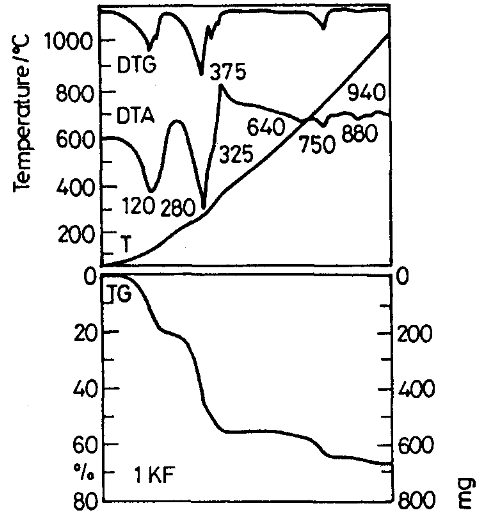

Fig. 14 DTA curve of the synthesis of topaz by sintering kaolinite-ammonium fluoride mix of a ratio of 1:1. Weight of sample 1000 mg, heating rate 10°C min^{-1}

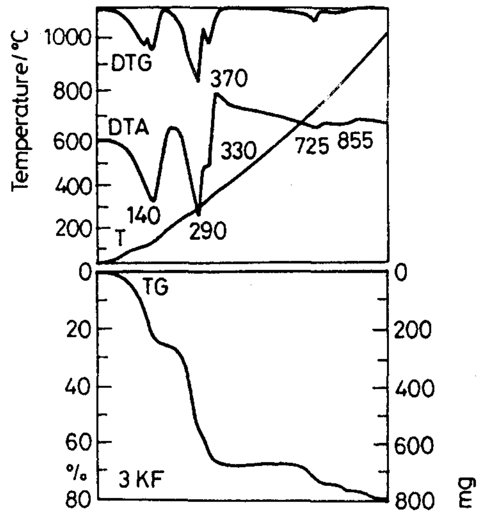

Fig. 15 DTA curve of the synthesis of topaz by sintering kaolinite-ammonium fluoride mix of a ratio of 1:1.7. Weight of sample 1000 & 184 mg, heating rate 10°C min^{-1}

220–240°C represents the dissociation of the resulted ammonium bifluoride and the unstable ammonium aluminium hexafluoride, yielding the more stable ammonium aluminium tetrafluoride. The large and sharp endothermic peak at 340–345°C represents the intensive dissociation of cryptohalite and ammonium aluminium tetrafluoride. These processes are connected with a sharp decrease in weight (TG curve), due to volatilization of silicon tetrafluoride and removal of ammonia and water vapours.

The intensive formation of topaz takes place at 770–800°C by an endothermic reaction. Topaz dissociates at 950°C (Fig. 11A) by an endothermic reaction and its simultaneous desilication occurs in the presence of an excess of aluminium fluoride, with the formation of corundum.

The X-ray diffraction patterns of the products of the runs at 155, 240, 345, 800 and 950°C are shown in Fig. 12. The product of the run at 155°C (Fig. 12A) consists mainly of ammonium aluminium hexafluoride and cryptohalite with some unreacted quartz. At 240°C (Fig. 12B), ammonium aluminium tetrafluoride and cryptohalite constitute the main components of the product. At 345°C (Fig. 12C), the product consists mainly of aluminium fluoride with some quartz due to the dissociation of ammonium aluminium tetrafluoride and cryptohalite. At 800°C (Fig. 12D), topaz constitutes the main component of the product with aluminium fluoride, while the product at 960°C (Fig. 12E) consists mainly of corundum with aluminium fluoride and some undissociated topaz.

Using mixes of a ratio of 1:1:2.5 (Fig. 11B) topaz dissociates at 1000°C, as indicated by the sharp endothermic peak, with the formation of mullite due to the deficiency of fluoride ions (Fig. 13).

The synthesis of topaz is assumed to proceed according to the following mechanism.

At 125–155°C: The reaction of corundum and quartz with ammonium fluoride takes place with the formation of ammonium aluminium hexafluoride and cryptohalite.

$$\underset{\text{corundum}}{Al_2O_3}+\underset{\text{quartz}}{SiO_2}+18NH_4F \rightarrow 2(NH_4)_3AlF_6+\underset{\text{cryptohalite}}{(NH_4)_2SiF_6}+10NH_3+5H_2$$

At 220–240°C: Ammonium aluminium hexafluoride is unstable and begins to decompose, yielding the more stable ammonium aluminium tetrafluoride.

$$(NH_4)_3AlF_6 \rightarrow NH_4AlF_4+2NH_3+2HF$$

At 340–345°C: Cryptohalite and ammonium aluminium tetrafluoride are unstable and dissociate according to:

$$(NH_4)_2SiF_6 \rightarrow SiF_4+2NH_3+2HF$$

$$NH_4AlF_4 \rightarrow AlF_3+NH_3+HF$$

Formation of topaz

At 770–800°C: The resulted aluminium fluoride reacts with quartz in the presence of water vapours with the formation of topaz.

$$\underset{\text{quartz}}{SiO_2}+2AlF_3+4H_2O \rightarrow \underset{\text{topaz}}{Al_2(SiO_4)(F,OH)_2}+4HF+H_2$$

Formation of corundum

At 950°C: Topaz dissociates in the presence of aluminium fluoride with simultaneous desilication; with the formation of corundum.

$$\underset{\text{topaz}}{Al_2(SiO_4)(F,OH)_2}+2AlF_3 \rightarrow \underset{\text{corundum}}{2Al_2O_3}+SiF_4+F_2+2HF$$

Formation of mullite

At 1000°C: In the absence of aluminium fluoride, topaz dissociates with the formation of mullite.

Synthesis of topaz by the sintering of kaolinite with ammonium fluoride

The DTA data of the sintering of kaolinite with ammonium fluoride for 1:1 mixes are shown in Fig. 14. The first two large and sharp endothermic peaks at 120 and 280°C represent the formation of ammonium aluminium hexafluoride and cryptohalite and their subsequent dissociation into ammonium aluminium tetrafluoride and silicon tetrafluoride and ammonia, respectively. The intensive formation of topaz takes place at 750°C. The small endothermic peak at 940°C represents the dissociation of topaz with the formation of corundum. The formation of mullite takes place at 1010°C. The end product of sintering consists mainly of mullite and some corundum at 1010°C, due to the deficiency of fluorine.

The DTA curve of kaolinite mixed with ammonium fluoride in a ratio of 1:1.7 (Fig. 15) shows similar peaks except the small peak at 855°C representing the loss of silicon tetrafluoride from topaz. Aluminium fluoride is the main constituent of the end product with some corundum and a few topaz and mullite grains.

The mechanism of topaz synthesis by the sintering of kaolinite with ammonium fluoride was found to be complicated and can be described as follows:
At 120°C: The reaction of kaolinite with ammonium fluoride takes place with the formation of ammonium aluminium hexafluoride and cryptohalite.

$$\underset{\text{kaolinite}}{Al_2Si_2O_5(OH)_4}+24NH_4F \rightarrow \underset{\text{cryptohalite}}{2(NH_4)_2SiF_6}+2(NH_4)_3AlF_6+14NH_3+9H_2O$$

At 290°C: Cryptohalite is unstable and dissociates with the liberation of ammonia, silicon tetrafluoride and water vapours or the reaction takes place according to:

$$\underset{\text{kaolinite}}{Al_2Si_2O_5(OH)_4}+16NH_4F \rightarrow 2NH_4AlF_4+2SiF_4+14NH_3+9H_2O$$

At 330°C: The dissociation of ammonium aluminium tetrafluoride takes place with the formation of aluminium fluoride.

$$\underset{\text{kaolinite}}{Al_2Si_2O_5(OH)_4}+14NH_4F \rightarrow 2AlF_3+2SiF_4+14NH_3+9H_2O$$

At 725–750°C: The reaction of kaolinite with aluminium fluoride takes place with the formation of topaz.

$$Al_2Si_2O_5(OH)_4+2AlF_3 \rightarrow Al_2(SiO_4)(F,OH)_2+Al_2O_3+SiF_4+H_2$$

kaolinite topaz corundum

At 940°C: The dissociation of topaz in the presence of excess aluminium fluoride takes place with the formation of corundum according to:

$$Al_2(SiO_4)(F,OH)_2+2AlF_3 \xrightarrow{940^\circ C} 2Al_2O_3+SiF_4+F_2+2HF$$

topaz corundum

At 1010°C: In the absence of aluminium fluoride, topaz dissociates with the formation of mullite according to:

$$Al_2(SiO_4)(F,OH)_2 \rightarrow 2Al_2O_3{\cdot}SiO_2+F_2+2OH$$

topaz mullite

Synthesis of topaz by the sintering of quartz with aluminium fluoride

The DTA data of the synthesis of topaz by the sintering of quartz with aluminium fluoride of an amount 150% of the theoretical value and using the theoretical amount are shown in Fig. 16A and B, respectively. The first two wide endothermic peaks at 140 and 330°C represent the dehydration of aluminium fluoride. The small endothermic peak at 550°C represents the transition of beta quartz to the alpha form and the beginning of the reaction between quartz and aluminium fluoride. The in-

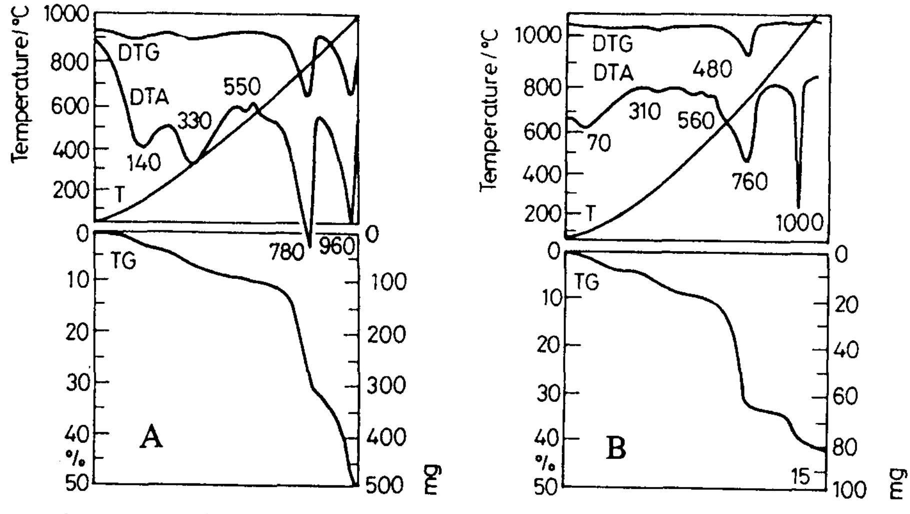

Fig. 16 DTA curve of the synthesis of topaz by sintering quartz with 150% of the theoretical amount of aluminium fluoride (A) and using the theoretical amount (B), respectively. Weight of sample 1000°C, heating rate 10°C min^{-1}

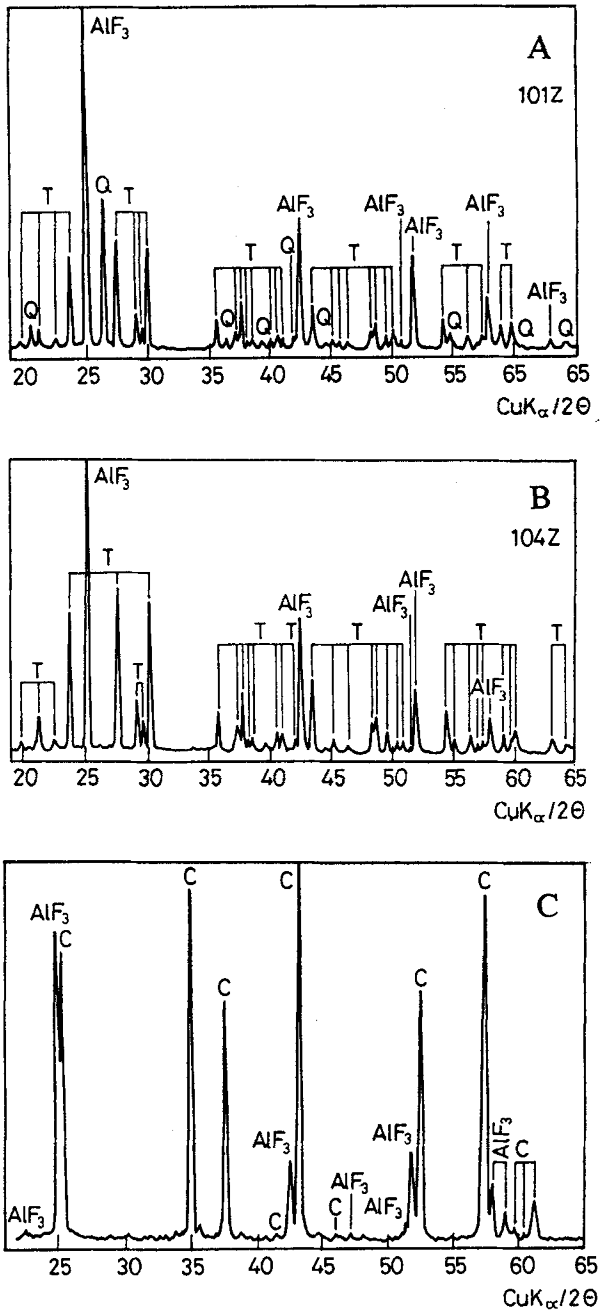

Fig. 17 X-ray powder diffraction patterns of the products of the synthesis of topaz by sintering quartz with 150% of the theoretical amount of aluminium fluoride (A), (B) and (C) at 550, 780 and 960°C, respectively. T=topaz, C=corundum and Q=quartz

tensive formation of topaz occurs at 780°C. This process is connected with a remarkable decrease in weight (TG curve) due to volatilization of silicon tetrafluoride. The resulting topaz dissociates with simultaneous desilication at 960°C by an endothermic reaction in the presence of excess aluminium fluoride, giving rise to corundum or alpha-aluminium oxide. This is also accompanied by a sharp decrease in sample weight due to the removal of silicon tetrafluoride and the loss of constitutional OH radicals.

The X-ray powder diffraction patterns of these products are shown in Fig. 17 (A at 550°C, B at 780°C and C at 960°C). Topaz is present in large amounts in the product of the run at 780°C and its peaks completely disappear in the run at 960°C.

DTA data of the synthesis of topaz by the sintering of quartz with theoretical amount of aluminium fluoride (Fig. 16B) indicate that the product of the reaction at 760°C is composed of topaz and unreacted quartz, indicating the incompleteness of the reaction of topaz formation. The sharp endothermic peak at 1000°C represents the dissociation of topaz with the formation of mullite as the end product, due to the deficiency of fluoride ions.

The produced topaz is colourless in thin sections, it has a high relief and weak birefringence with perfect basal (001) cleavage and crystallizes in the orthorhombic system in the form of prismatic crystals and is optically positive.

Synthesis of perovskite

Perovskite ($CaTiO_3$) occurs as an accessory mineral in basic and alkaline igneous rocks. Also, it is found in some impure contact metamorphosed limestones [5, 21]. Perovskite is one of the components of titanium slags, obtained from the smelting of ilmenite [17, 22]. Processing of ilmenite by smelting is used for the en-

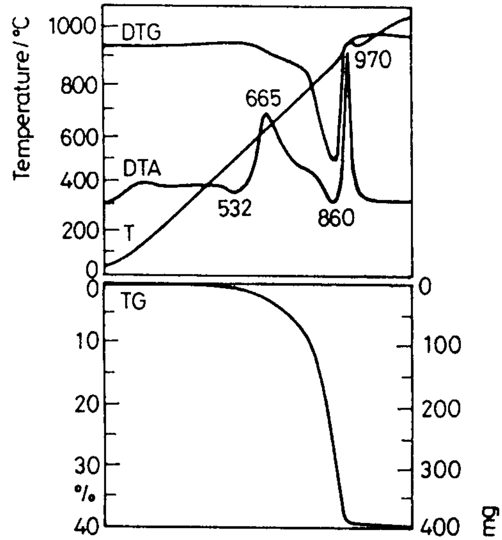

Fig. 18 DTA curve of the synthesis of perovskite by sintering rutile with calcite. Weight of sample 1000 mg, heating rate 10°C min^{-1}

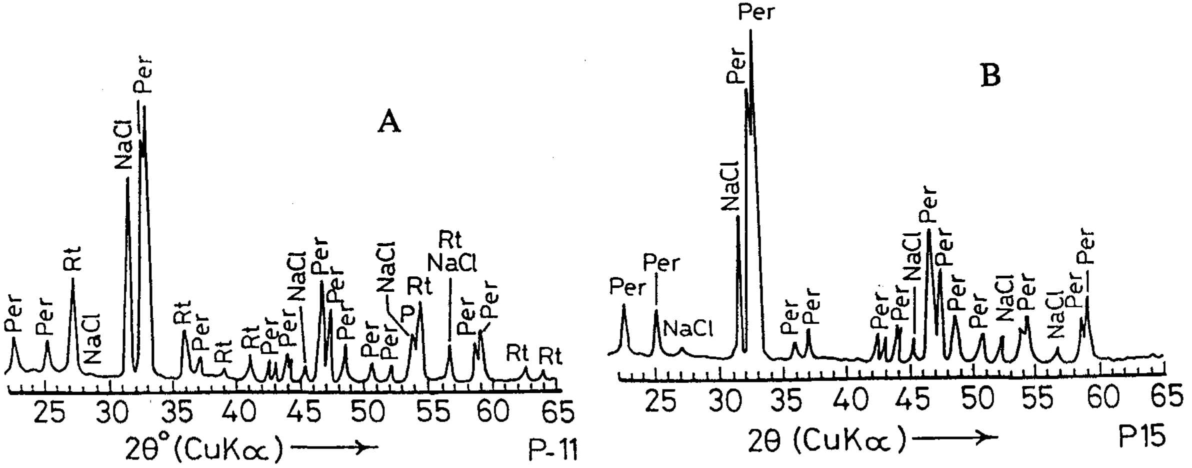

Fig. 19 X-ray powder diffraction patterns of the products of synthesis of perovskite by sintering rutile with calcite (A) & (B) at 665 and 970°C, respectively. Rt. = rutile; Per. = perovskite

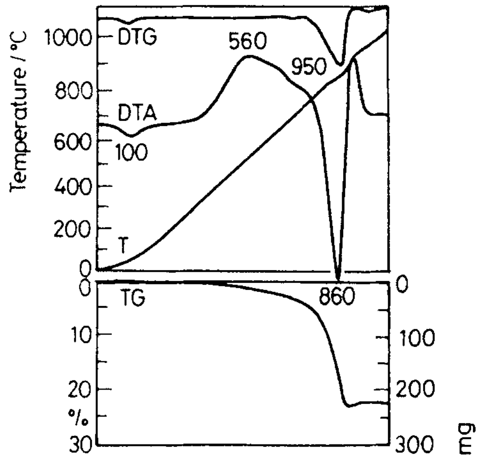

Fig. 20 DTA curve of the synthesis of perovskite by sintering ilmenite with calcite. Weight of sample 1000 mg, heating rate 10°C min^{-1}

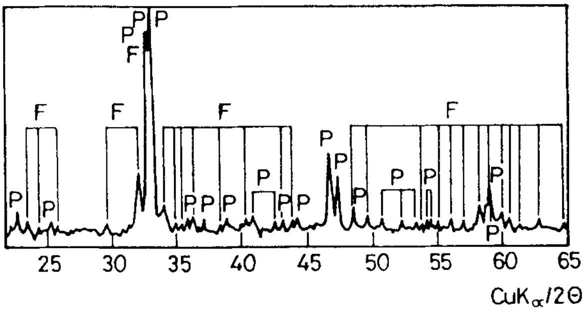

Fig. 21 X-ray powder diffraction pattern of the products of synthesis of perovskite by sintering ilmenite with calcite at 950°C. P=perovskite; F=calcium ferrite

richment of titanium in the low grade titaniferous iron ores. Smelting of ilmenite with coke is carried out at 1100–1150°C in the presence of fluxes (limestone or lime, magnesite and soda). Smelting results in the production of cast iron and titanium rich slags containing 70–80% TiO_2 in the form of perovskite [17, 22].

Synthesis of perovskite by the sintering of rutile with calcite

The DTA curve of rutile mixed with calcite and graphite in a ratio of 1:2:0.1 is shown in Fig. 18. The large exothermic peak at 665°C represents the burning of graphite and the combustion of volatiles. The large endothermic peak at 860°C represents an intensive dissociation of calcite and probably a reaction between the resulted calcium oxide and rutile. This process is connected with a remarkable decrease in weight (TG curve) due to the removal of carbon dioxide. The large and sharp exothermic peak at 970°C represents the intensive reaction between rutile and the dissociated calcite with the formation of perovskite. An X-ray diffraction study of the products of sintering showed the first appearance of perovskite above 665°C (Fig. 19A). The X-ray powder diffraction pattern of the end product of sintering at 970°C (Fig. 19B) shows only the narrow and intense X-ray peaks of perovskite, indicating the completeness of the reaction.

Synthesis of perovskite by the sintering of ilmenite with calcite

Thermal studies of the synthesis of perovskite by the sintering of ilmenite with calcite in the presence of graphite (Fig. 20) show the intensive formation of perovskite at 950°C in an exothermic reaction between ilmenite and dissociated calcite. The X-ray diffraction pattern of the product at 950°C (Fig 21) shows the intense and large peaks of perovskite and calcium ferrite of the composition $Ca_2Fe_2O_5$. The ilmenite peaks disappear completely, indicating its complete conversion to perovskite.

The synthesized perovskite is colourless in thin sections and has high relief, weak pleochroism and weak birefringence.

Synthesis of scheelite

Scheelite ($CaWO_4$) occurs in contact metamorphosed deposits, hydrothermal veins and pegmatites. Scheelite is also the product of roasting of wolframite with calcium oxide or limestone or its fusion with calcium chloride, followed by acid treatment of calcium tungstate [17, 21, 22].

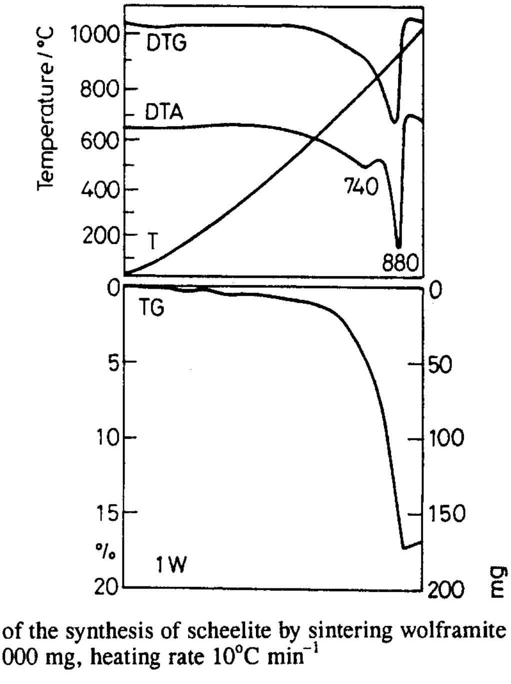

Fig. 22 DTA curve of the synthesis of scheelite by sintering wolframite with calcite. Weight of sample 1000 mg, heating rate 10°C min^{-1}

Synthesis of scheelite from wolframite by sintering with calcite

The DTA curve of the sintering of wolframite with theoretical amount of calcite (Fig. 22) shows the beginning of the reaction at 550°C with the formation of scheelite. The intensive formation of scheelite occurs at 740°C. This is closely followed by the dissociation of unreacted calcite as represented by the large and sharp endothermic peak at 880°C. These processes are connected with a sharp decrease in sample weight (TG curve) due to the removal of carbon dioxide.

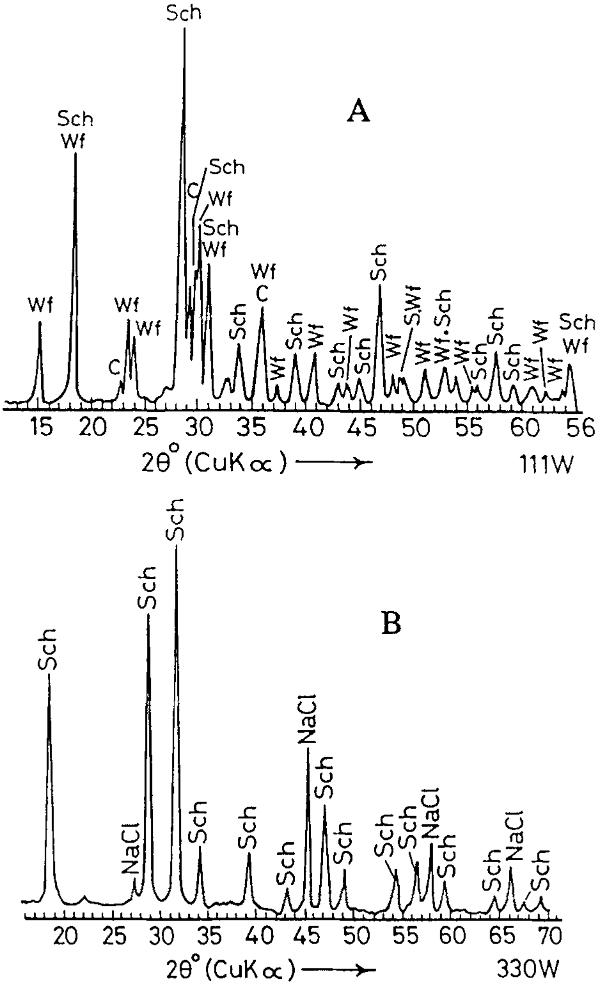

Fig. 23 X-ray powder diffraction patterns of the products of synthesis of scheelite by sintering wolframite with calcite. (A) & (B) at temperatures 550 and 740°C, respectively. Sch. = scheelite; Wf. = wolframite and C = calcite

The X-ray diffraction patterns of the products of sintering (Fig. 23A and B) show the appearance of scheelite at 550°C with unreacted wolframite. The pattern of the end product at 740°C (Fig. 23B) shows only the large, narrow and intense peaks of scheelite, indicating completeness of the reaction.

The resulted scheelite is colourless in thin sections, crystallizing in the tetragonal system in the form of tabular crystals with distinct cleavage (101) and is optically positive.

The unit cell dimensions, constants and optical axial angles of the synthesized minerals, namely, baddeleyite, corundum, topaz, wulfenite, perovskite and scheelite (Table 1) are consistent with the corresponding data of the natural minerals.

Table 1 Unit cell dimensions and axial angles of the synthesized minerals

Mineral	*a*/	*b*/	*c*/	α/	β/	γ/	*V*/
		Å			C° min^{-1}		Å^3
Baddeleyite		(Monoclinic)					
Synthetic	5.2458	5.2030	5.2849	90.00	80°48′	90.00	142.26
	±0.0611	±0.0769	±0.0722	0.00	±1.051	0.00	±0.01
Standard	5.26	5.21	5.37	90.00	80°36′	90.00	145.102
Corundum		(Trigonal)					
Synthetic	4.7424	4.7424	12.9807	90.00	90.00	120.00	252.83
	±0.0109	±0.0109	±0.02091	0.00	0.00	0.00	±0.004
Standard	4.751	4.751	12.98	90.00	90.00	120.00	253.725
Wulfenite		(Tetragonal)					
Synthetic	5.4268	5.4268	12.1043	90.00	90.00	90.00	356.474
	±0.0107	±0.0107	±0.0208	0.00	0.00	0.00	±0.003
Standard	5.435	5.435	12.11	90.00	90.00	90.00	357.72
Topaz		(Orthorhombic)					
Synthetic	4.638	8.767	8.378	90.00	90.00	90.00	340.661
	±0.0154	±0.0313	±0.0251	0.00	0.00	0.00	±0.004
Standard	4.649	8.792	8.394	90.00	90.00	90.00	343.096
Perovskite		(Pseudocubic)					
Synthetic	7.6389	7.6632	7.6877	90.00	90.00	90.00	450.026
	±0.0514	±0.0445	±0.0323	0.00	0.00	0.00	±0.325
Standard	7.65	7.65	7.65	90.00	90°40′	90.00	447.697
Scheelite		(Tetragonal)					
Synthetic	5.2376	5.2376	11.3458	90.00	90.00	90.00	311.243
	±0.0113	±0.0113	±0.0103	0.00	0.00	0.00	±0.214
Standard	5.246	5.246	11.349	90.00	90.00	90.00	312.330

Conclusions

Differential thermal analysis (DTA) and thermogravimetry (TG) are proved to be important and valuable tools in mineral synthesis for studying the reaction mechanism of the starting materials, optimum temperature of synthesis, the thermal behaviour of minerals and their physical and chemical transformations at different temperatures. From this DTA study the following conclusions may be drawn:

1) Topaz can be synthesized from different starting materials (kaolinite and aluminium fluoride, corundum-quartz mix with ammonium fluoride, kaolinite and ammonium fluoride, and quartz-aluminium fluoride mix). The intensive formation of topaz takes place at 750–800°C. Topaz dissociates at 1000–1010°C with the formation of mullite. In the presence of fluoride ions, dissociation and simultaneous desilication of topaz takes place at 940–960°C with the formation of corundum.

2) The DTA curves of the synthesis of the refractory materials baddeleyite and corundum by the sintering of zircon with aluminium fluoride show its formation to occur at 820°C.

3) The DTA curves of the synthesis of cryptohalite by sintering quartz with ammonium fluoride show its formation to occur at 125–155°C. Cryptohalite is unstable and dissociates at 320–335°C.

4) The DTA curves of the synthesis of wulfenite by sintering cerussite or lead oxide with molybdite show its formation to occur at 500–520°C.

5) The DTA curves of the synthesis of perovskite by sintering rutile or ilmenite with calcite in the presence of graphite show its formation to occur at 950°C.

6) The DTA curves of the synthesis of scheelite by sintering wolframite with calcite show its formation to occur at 550–740°C.

References

1 A. M. Abdel Rehim, Proc. 4th ICTA Vol. 1 Budapest 1974, p. 523.
2 A. M. Abdel Rehim, Acta Geol. Acad Sci. Hung., 19 (1975) 287.
3 A. M. Abdel Rehim, Thermochim. Acta, 13 (1975) 231.
4 A. M. Abdel Rehim, Acta Mineralogica-Petrographica, Szeged, Hungary, 22 (1976) 352.
5 A. M. Abdel Rehim, Acta Geol. Acad. Sci. Hung., 20 (1976) 19.
6 A. M. Abdel Rehim, Thermochim. Acta, 30 (1979) 127.
7 A. M. Abdel Rehim, Proc. 6th ICTA, Bayreuth, Germany, Birkhäuser-Verlag, Vol. 1, 1980.
8 A. M. Abdel Rehim, Proc. 7th ICTA, Kingston, Ontario, Canada, 1982.
9 A. M. Abdel Rehim, Application of Thermal Analysis in Mineral Technology, in: Thermal Analysis in the Geosciences, (Eds) W. Smykatz-Kloss and S. St. Warne, Springer-Verlag 1991, p. 188.
10 A. M. Abdel Rehim, J. Thermal Anal., 38 (1992) 475.
11 A. M. Abdel Rehim, J. Thermal Anal., 46 (1996) 193.
12 A. Blazek, Thermal Analysis, Van Nostrand Reinhold Co., 1973.
13 A. Bien and W. L. Dekeyser, Clay Min. Bull., 5 (1962) 80.
14 B. Locsei, Proc. 9th silicate Industry, Budapest, 1968, p. 103.
15 F. M. Luskotov, Metallurgy of Lead and Zinc, Metallurgia Publ., 1965.
16 R. C. Mackenzie, 'Scifax' Differential Thermal Analysis Data Index, Cleaver Hume Press, London 1962.

17 G. A. Mirson and A. N. Zelikman, Metallurgy of Rare Metals, Metallurgia Publ., Moscow 1965.
18 W. Smykatz-Kloss, Differential Thermal Analysis, Application and Results in Mineralogy. Minerals and Rocks, Vol. 11, Springer Verlag 1974.
19 A. A. Opalovsky, V. E. Fedorov and T. D. Fedotova, J. Thermal Anal., 5 (1973) 475.
20 F. Paulik, J. Paulik and L. Erdey, Talanta, 13 (1966) 1405.
21 Wm. R. Phillips and D. T. Griffen, Optical Mineralogy. The Nonopaque Minerals, W. H. Freeman and Company, 1981, p. 402.
22 A. N. Zelikman, O. E. Krein and G. V. Samsonov, Metallurgy of Rare Metals, Metallurgia Publ., Moscow 1964.